

Experimental feasibility of measuring the gravitational redshift of light using dispersion in optical fibers

S. Manly, E. Page

Department of Physics and Astronomy

University of Rochester

(June 8, 2024)

$$\nu' \approx \nu \left\{ 1 \pm \frac{gz}{c^2} \right\} \quad (1)$$

This paper describes a new class of experiments that use dispersion in optical fibers to convert the gravitational frequency shift of light into a measurable phase shift or time delay. Two conceptual models are explored. In the first model, long counter-propagating pulses are used in a vertical fiber optic Sagnac interferometer. The second model uses optical solitons in vertically separated fiber optic storage rings. We discuss the feasibility of using such an instrument to make a high precision measurement of the gravitational frequency shift of light.

04.80.Cc, 42.81.D, 42.25.H

I. INTRODUCTION

Einstein's Equivalence Principle (EEP) is the pillar underlying all metric theories of gravity, including the theory of general relativity. This principle states that effects of a uniform gravitational field are identical to the effects of uniform acceleration of a coordinate system. EEP can be decomposed into three components: the weak equivalence principle, local Lorentz invariance, and local position invariance (LPI). Precision experiments testing each of these components have yielded results consistent with EEP and the theory of general relativity [1] [2]. However, it is interesting to note that current solar and atmospheric neutrino data are consistent with a small violation of EEP [3]. Given the fundamental nature of EEP, higher precision tests are desirable. Such experiments might rule out some metric theories of gravity, uncover a deviation from our expectation that would require a modification of our current view of gravity, and place constraints on new macroscopic forces (which might be perverse enough to respect the weak equivalence principle, but not LPI) [4].

Local position invariance requires the results of local nongravitational experiments to be independent of position and time. Limits on violations of LPI have been set by searching for variation in the 'constants' of nature and by gravitational redshift experiments [1]. To date, all experimental results are consistent with LPI.

In a uniform gravitational field with strength g , the frequency shift of light traveling a distance z along the direction of maximum field gradient is given by

to first order, where the negative sign is used for light traveling against the gravitational field and the positive sign is used for light traveling with the field. Experiments that measure the gravitational frequency shift of light report results as a limit on the deviation observed from the equation above. The deviation, α , is defined by

$$\frac{\Delta\nu}{\nu} = (1 + \alpha) \frac{\Delta U}{c^2}, \quad (2)$$

where ΔU is the change in gravitational potential (gz in the example above) encountered by the light. Currently, the best limit on α comes from a 1976 experiment that compared the frequency of a precision hydrogen maser frequency standard on the surface of the earth with one launched by a Scout Rocket to a height of approximately 10,000 km. This experiment yielded a result of $\alpha < 2 \times 10^{-4}$ [5].

II. A NEW CLASS OF EXPERIMENTS

Continuous wave light will travel a vertical distance h in an optical fiber with index of refraction n in a time

$$t = \frac{h}{c} n \quad (3)$$

The frequency dependence of this flight time is given by

$$dt = \frac{h}{c} \left(\frac{dn}{d\nu} \right) d\nu. \quad (4)$$

Assuming this to take place near the earth's surface (let g be constant), the change in the gravitational potential over a distance dh induces a frequency change

$$d\nu = \frac{g\nu}{c^2} dh. \quad (5)$$

Over a height h , the flight time of the light will differ from that given by equation (3) by an amount

$$\delta t = \frac{g\nu h^2}{2c^3} \left(\frac{dn}{d\nu} \right), \quad (6)$$

Assuming a sinusoidal form for the light waves traveling down the fiber optic cable of

$$e^{i(\beta z - \omega t)} \quad (7)$$

the phase can then be written as

$$\phi = \beta(\omega)z - \omega t \quad (8)$$

where

$$\beta = \frac{n\omega}{c}. \quad (9)$$

The phase variation becomes

$$\delta\phi = (\delta\beta)z + \beta\delta z - (\delta\omega)t - \omega\delta t. \quad (10)$$

Specializing to our case, z become the height difference, h , and since this is a constant in our proposal, the variation of h is zero and the second term in the above equation disappears. Now the propagation parameter, β can be expanded, to first order as

$$\beta(\omega) = \beta_0(\omega_0) + \beta_1(\omega_0)\Delta\omega + \dots \quad (11)$$

Keeping the first order term in the variation and substituting this and our previously derived equations for the t 's into the phase equation above, we get

$$\delta\phi = \beta_1\delta\omega h - \frac{nh}{c}\delta\omega - \omega\frac{g\omega h^2}{2c^3}\frac{dn}{d\omega} \quad (12)$$

From the definitions above

$$\beta_1 = \frac{d\beta}{d\omega} = \frac{\omega}{c}\frac{dn}{d\omega} + \frac{n}{c} \quad (13)$$

Using this in the above result for $\delta\phi$ gives

$$\delta\phi = \frac{g\omega}{c^2}h\left(\frac{\omega}{c}\frac{dn}{d\omega}h + \frac{nh}{c} - \frac{nh}{c}\right) - \omega\frac{g\omega h^2}{2c^3}\frac{dn}{d\omega} \quad (14)$$

and

$$\delta\varphi = \frac{\pi g\nu^2 h^2}{nc^3} \left(\frac{dn}{d\nu}\right). \quad (15)$$

In principle, this phase shift can be measured relative to light traveling through a fiber with different dispersion to determine or place a limit on α in equation (2). Alternatively, the information could be used to make a measurement of g . In fact, a net phase shift can be preserved while the light is returned to the original height by making the return path out of fiber with a different dispersion, as shown in Figure 1. Unfortunately, the phase shift expected per unit length of fiber is small for reasonable values of dispersion, making it necessary to have a relatively long path length to produce a measurable effect. The experimental difficulty is to maintain sufficient light at the end of the path to make a measurement while preserving the phase shift or timing well enough to make the measurement meaningful.

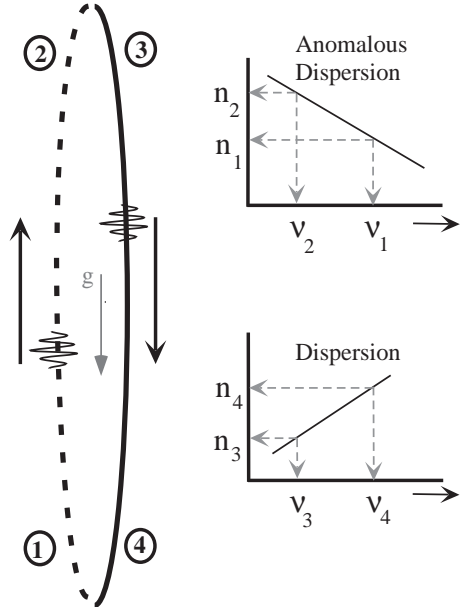


FIG. 1. Diagram illustrating the interplay of the gravitational frequency shift of light and dispersion.

We have considered two experimental models in evaluating the feasibility of a high precision measurement of the gravitational redshift of light using this effect. The first uses long counter-propagating pulses in a vertical fiber optic Sagnac interferometer. The second model uses optical solitons propagating in two vertically separated fiber optic storage rings. In spite of being less conventional, the latter approach presents fewer technical challenges and is more likely to yield a robust measurement.

III. EXPERIMENTAL MODEL OF VERTICAL FIBER OPTIC SAGNAC INTERFEROMETER WITH VARYING DISPERSION

Coherent light traveling from a source is split into two beams that travel in opposite directions around a loop or coil of optical fiber. After traversing the coil, the two beams of light are recombined and the phase difference between the clockwise (CW) and counter-clockwise (CCW) beams is measured. This technique is used widely to make high precision fiber optic gyroscopes (FOG) that make use of the fact that a phase difference between the two paths is induced by a rotation of the coil [6]. In our model, the coil lies in a vertical plane. Unlike the FOG, the fiber dispersion must vary asymmetrically around the circumference of the loop in order yield a net phase shift due to the interplay of dispersion and the gravitational frequency shift. At the top and bottom of each loop in the coil are splices to join the fibers of differing dispersion. The pattern of varying dispersion is such that the CW (CCW) beam always travels upward

Signal vs. Pathlength for Different Loop Heights (Analytical)

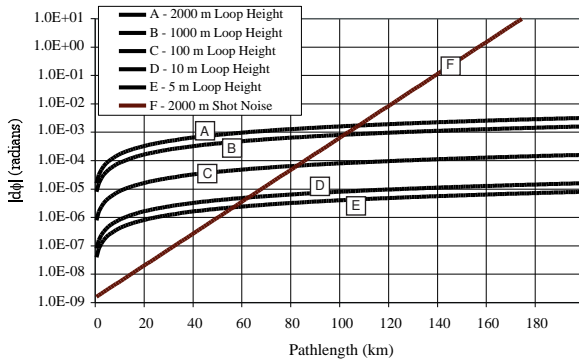


FIG. 2. Signal size versus path length for various loop heights along with the shot noise for a 2000 meter loop. (Results from an analytical calculation.)

through fiber with positive dispersion and downward through fiber with negative or anomalous dispersion. The situation is reversed for the CCW (CW) beam.

As the CW and CCW beams propagate through the coil, a phase difference between the beams develops with time due to the gravitational frequency shift. This phase difference is given by

$$\delta\varphi = \frac{2\pi N g h^2 \nu^2}{nc^3} \left[\left(\frac{dn}{d\nu} \right)_L - \left(\frac{dn}{d\nu} \right)_R \right] \quad (16)$$

for beams of initial frequency ν , traveling N turns around a loop of height h in a uniform gravitational field with strength g . The dispersion on one side of the fiber loop is $(dn/d\nu)_L$ while that on the other side is $(dn/d\nu)_R$.

At 1550 nm, for an interferometer constructed of fibers with dispersion $+15$ ps/nm-km ($=3.7 \times 10^{-17}$ s) and -90 ps/nm-km ($=-2.2 \times 10^{-16}$ s), respectively, and setting $n=1.5$, equation (8) becomes

$$\delta\varphi = (1.6 \times 10^{-11}) N h^2. \quad (17)$$

Figure 2 shows the size of the phase shift as a function of total path length and loop height. Although many sources of noise need to be considered, the measurement precision is limited ultimately by light loss in the fiber and at the splices.

In order to estimate, roughly, the potential sensitivity of such an experiment, it is necessary to fold in the shot noise. The photon counting noise in the phase can be estimated by the Heisenberg uncertainty principle as

$$(\delta\varphi)_{shot} \approx \frac{1}{\sqrt{N_{photons}}}. \quad (18)$$

For a 10 mW laser source operating at 1550 nm, this estimate becomes

$$(\delta\varphi)_{shot} = \frac{1}{\sqrt{(5 \times 10^{17}) t e^{-\alpha d}}}, \quad (19)$$

Signal vs. Pathlength for Different Loop Heights (Numerical)

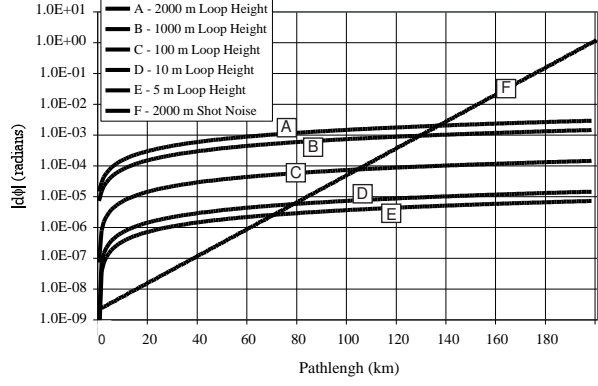


FIG. 3. Signal size versus path length for various loop heights along with the shot noise for a 2000 meter loop. (Results from a numerical calculation.)

where t is the signal integration time (in s), α is the total fiber light loss (in dB/km), and d is the total distance traveled by the light (in km). Assuming a fiber light loss of 0.5 dB/km and a loss at each splice of 0.5 dB yields the shot noise limit shown in Figure 2.

The results in figure 2 are from analytical calculations. We have also used the split step Fourier method to solve the non-linear Schrodinger equation for this model numerically [7]. The results, shown in Figure 3, are very similar to those obtained by analytical calculations. The difference in the shot noise curve comes about because the analytical model treats the light loss at splices as a continuous process, while the numerical model incorporates discrete losses at the splices and should be more accurate.

Things besides shot noise can limit the sensitivity of this experiment. Source relative intensity noise, thermal fluctuations, changing mechanical stresses, polarization mode cross coupling, and coherent backscattering at the splices can lead to nonreciprocal phase shifts.

Signal to Noise Ratio (With Noise Floor)

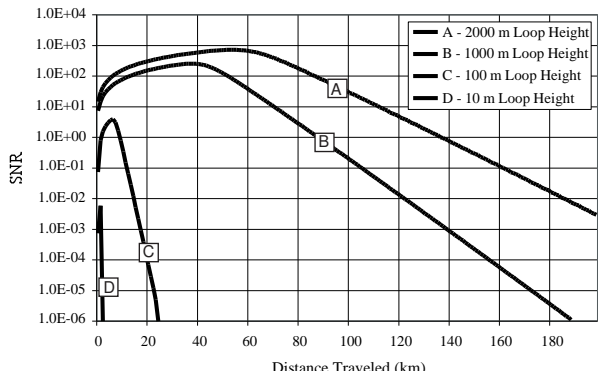


FIG. 4. Signal to noise ratio, assuming a noise floor at 1 μ rad and shot noise.

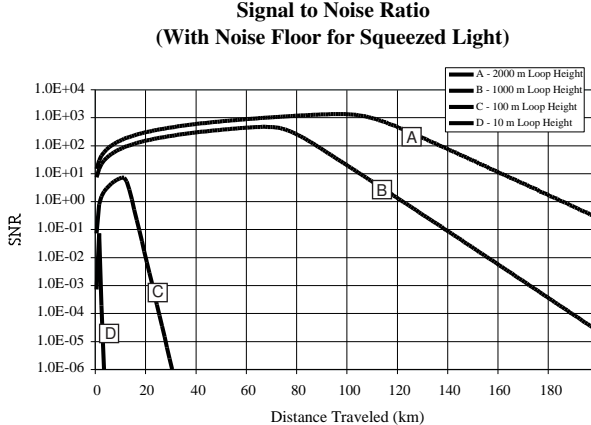


FIG. 5. Signal to noise ratio for the Sagnac interferometer model with various loop heights and a 1 mrad noise floor. The shot noise included in this calculation is reduced by a factor of 100, relative to Figure 4, as an optimistic assessment of the effect of using squeezed light.

In addition, electronics noise can be an issue. Without constructing a very detailed model and/or building prototypes, it is difficult to estimate the level of these sources of noise in this experimental model. One useful point of comparison is the fiber optic gyro, mentioned earlier. The FOG is a continuous wave fiber Sagnac interferometer that is vulnerable to many of the same sources of noise. Very high sensitivity FOGs are sensitive to a rotation-induced phase change of 1×10^{-9} radians. A sensitivity of one μrad is considered difficult, but achievable [6] [8].

Figure 4 shows the signal-to-noise ratio for this model with varying loop height, shot noise and a 1 μrad noise floor. Without using squeezed light, the shot noise provides a hard cutoff in the path length for a given loop height. An optimistic estimate of what could be done using squeezed light is shown in Figure 5. For this curve, the shot noise is reduced by a factor of 100 [9].

In our view, Figures 4 and 4 represent an optimistic assessment of what might be achievable with current technology. Our model differs from a FOG in some very significant ways. FOG designers struggle to maintain reciprocity between the counter propagating beams in order to achieve the high sensitivity of the best instruments. Non-reciprocal dispersion is a necessary component of this model. In addition, FOGs are wound about titanium cores in a carefully maintained and monitored environment. In our model, the loop necessarily extends a large vertical distance, which would complicate attempts at noise reduction.

Another weakness of this model is that it would be very difficult to make a differential measurement, which would be helpful for extracting the signal. It is hard to imagine being able to rotate the device or change the height without causing arbitrary phase changes between the counter-propagating beams. The growth of the phase shift with time, compared in different orientations, would be the best way to pull out the signal. This is another

place where our model differs significantly from the FOG. FOGs work with continuous wave light and our model requires long pulses.

To summarize our work on this model, it is conceivable that a high precision measurement of the gravitational redshift of light could be made using a vertical fiber Sagnac interferometer with varying dispersion. However, the technical difficulties are challenging and further modeling and prototyping would be useful in evaluating the eventual sensitivity that might be achieved.

IV. EXPERIMENTAL CONCEPT: VERTICALLY SEPARATED OPTICAL SOLITON STORAGE RINGS

A coherent beam of light pulses is split into two streams, each of which is transformed into a bitstream of solitons [10]. The streams are injected and stored for a period in separate fiber optic storage loops [11] sitting at different gravitational potentials. The group velocity of the solitons in the two storage rings will differ due to the interplay of dispersion with the gravitationally-induced change in the carrier frequency of the solitons. Unfortunately, the substantial timing jitter that normally accompanies solitons in storage rings makes it impractical to measure directly the relative quantum phase difference between the two beams. Rather, a relative net timing difference between the pulses in the two beams will develop over time, which is proportional to the gravitational frequency shift of the light. This timing difference is used to measure, or place a limit, on α . The troublesome shot noise limit is avoided by the use of amplification in the storage ring.

A. Conceptual details

Consider an optical pulse that is split into two coherent pulses with the same intensity profile. Let one travel horizontally for a distance h and the other travel vertically a distance h . The group velocity dispersion parameter β_2 for each pulse is given by

$$\beta_2 = -\frac{1}{2\pi} \frac{dv_g}{d\nu}, \quad (20)$$

where v_g is the group velocity of the carrier frequency of the pulse [12]. Assuming the fiber to be identical for each path, there is a gravitationally-induced group velocity difference,

$$|\Delta v_g| = \Delta\nu \left(\frac{dv_g}{d\nu} \right) = 2\pi\beta_2 \frac{gh\nu}{c^2}, \quad (21)$$

between the pulses as they reach the end of their respective paths, where g is assumed constant over the height difference. (In practice, the variation in g must be measured and taken into account.) At this point, if the

pulse streams were each allowed to travel a horizontal distance d along identical fibers and then recombined (in such a manner that the path lengths were identical), there would be a relative pulse timing difference between the pulses [13]. Unfortunately, the effect is quite small for reasonable input parameters and practical distances.

One way of increasing the size of the effect is to increase the distance d . In this model, that is done by using optical soliton pulses and injecting each stream of pulses into ‘identical’ fiber optic storage loops, where amplification is provided by erbium doped fiber amplifiers (EDFA’s). The soliton character prevents dispersion from destroying the pulses, while amplified spontaneous emission noise is controlled using amplitude modulation, and pulse timing jitter is reduced with frequency filtering. This model is schematically illustrated in Figure 6. This and similar techniques for pulse memory and storage and long-haul transmission have been studied extensively in the last decade [11]. A scheme similar to what we are proposing was used in 1993 to store a 10 GHz bit pattern for distances up to 180×10^6 km (storage times of 15 minutes), as described in reference [14]. The authors of that work conclude, “error free transmission over unlimited distances is possible with this technique.”

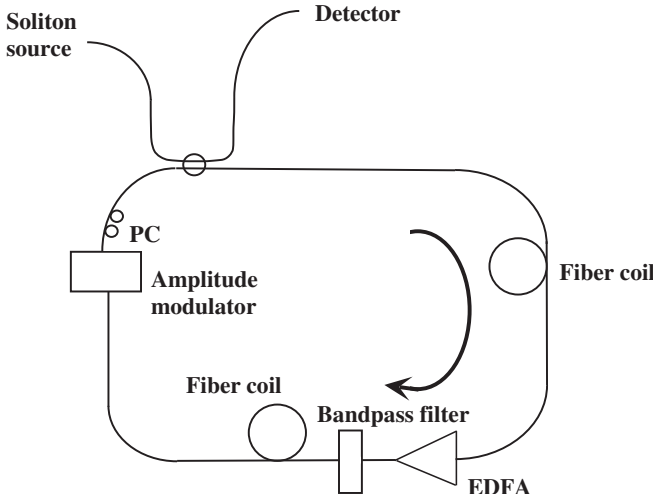


FIG. 6. The basic components of a fiber optic storage loop.

The goal of the telecommunications and pulse storage research on optical storage loops is to preserve the information, i.e., a high rate bit pattern, over time and distance. Our goal is somewhat broader, as we want to preserve the bit pattern *as well as* a small relative overall group velocity difference between the bits in two separate streams. If preserved over time, this relative group velocity difference will be translated into a measurable pulse timing difference. There are sources of random pulse timing jitter, as we will discuss below. However, these noise sources will cause the solitons to random walk in relative timing, while the gravitationally-induced relative velocity difference should provide a small, but inexorable, bias in one direction. There are other effects

(as discussed below) which can cause a unidirectional shift in the group velocity of the solitons. In this model, the gravitationally-induced effect is pulled out from the background through differential measurements of the relative pulse timing between configurations with loops at different heights.

Figure 6 shows the basic components of a soliton storage ring experiment. Soliton pulses are used because these solutions to the nonlinear Schrödinger equation balance dispersion against the non-linear Kerr effect, and yield a pulse that is largely immune to dispersive effects in the fiber. Light loss due to scattering is replaced with continuous or lumped amplification by EDFA’s. Synchronous amplitude modulation limits the growth of amplified spontaneous noise that would otherwise overwhelm the signal, and a frequency filter is used in concert with the modulator to stabilize the pulse from amplitude and width fluctuations.

B. Noise sources

There are numerous things that can effect the pulse timing in such an optical storage loop.

• Gordon-Haus Jitter

All optical amplifiers introduce noise into the system by amplified spontaneous emission (ASE). In non-linear fiber optics, this ASE noise is also called Gordon-Haus Jitter. When an optical amplifier introduces ASE, the pulse undergoes small amplitude and phase fluctuations at the amplifier output, which lead to a change in the carrier frequency, and therefore the group velocity of the pulse. Over a span of fiber optic cable, this leads to a random jitter in the timing of the soliton pulse. The effect of this jitter on soliton stream transmission has been quantified as [12] [15]

$$BL_T < \left[\frac{\pi f_j^2}{q_0 \lambda h \alpha \gamma D} \right]^{1/3}, \quad (22)$$

where B is the bit rate, L_T is the length traveled, f_j is the fraction of the bit slot that the error should be smaller than, q_0 is the initial soliton separation in normalized units, λ is the wavelength of light, α is the attenuation coefficient, γ is the nonlinearity coefficient, and D is the dispersion coefficient.

Agrawal gives an illustrative example in reference [12]. A system using 1550 nm light with $q_0 = 10$, $\alpha = 0.2 \text{ dB/km}$, $\gamma = 10 \text{ W}^{-1}/\text{km}$, and $D = 2 \text{ ps}/(\text{nm-km})$, and assuming $f_j = 0.2$ for tolerable jitter. leads to

$$BL_T < 34,000(\text{Gb/s}) - \text{km}. \quad (23)$$

A 10 Gbit/s system is limited to a transmission length of 3400 km in this example. This length is

small compared to the soliton transmission lengths required by our experiment.

Fortunately, there are a number of ways to overcome this bit-length limitation [11] [12] [14] [16], including the use of optical filters and external modulators. Filters reduce the overall noise level by eliminating the ASE-noise outside the filter bandwidth and synchronous modulation forces the soliton to realign itself within the bit slot. Both techniques reduce the jitter, and when used together properly, can lead to an unlimited propagation distance.

- **Raman Self Frequency Shift (RSFS)**

As the soliton pulse travels down a fiber optic cable, the photons scatter off of atoms in the cable. In the process, some of the photon energy can be lost to atomic vibrational modes, yielding an outgoing photon frequency that is lower than that of the incoming photon. This effect, known as the Raman effect, causes a continuous flow of energy from the high frequency part of the soliton pulse to the low frequency part of the pulse. Thus, there is a downshift in the carrier frequency of the soliton as it moves along the cable, which effects the group velocity of the soliton and could give a relative timing difference in our experiment if the effect is asymmetric between the two rings [12] [17] [18].

It is well known that a light pulse and its frequency range are related to each other via the Fourier transform. Therefore, the shorter the soliton pulse, the wider its frequency range. Solitons of ~ 1 ps or less have a wide enough frequency range that the frequency shift of the soliton due to the Raman effect is very noticeable. Models have shown [17] that the redshift associated with the soliton scales T_0^{-4} , where T_0 is the soliton pulse width. So, the noticeable effect drops off quickly for pulse widths above 1 ps. This is an important design consideration in our experiment.

- **Soliton Interactions**

The same non-linearity that causes solitons to be stable also causes an interaction force between solitons. The interaction force between solitons depends on the separation of the solitons, their relative amplitude, and their relative phase [12]. Only in the case of two solitons with the same relative phase is the soliton-soliton interaction attractive. In all other cases, where the solitons have a different relative phase, the interaction force is repulsive. In the specific case when the relative phase $\theta = 0$ and the relative amplitude $r = 1$, the relationship between soliton separation and distance traveled down a fiber optic cable is given by

$$\exp[2(q - q_0)] = \frac{1}{2}[1 + \cos(4\xi e^{-q_0})], \quad (24)$$

where q_0 is the initial soliton separation, and q is the soliton separation at a distance ξ along the fiber. From this equation it can be seen that the solitons periodically combine and then separate once again with a period ξ_p , given by [19]

$$\xi_p = \frac{\pi \sinh(2q_0) \cosh(2q_0)}{2q_0 + \sinh(2q_0)}. \quad (25)$$

It is important to note the interaction force drops exponentially with the distance between solitons.

Soliton interactions for two solitons, three solitons, and a random sequence of solitons have been studied numerically [20]. It was found that in a given soliton stream with a number of consecutive bits filled, it only the first and last solitons of the consecutive bit stream are effected by the soliton interaction because the interior solitons experience approximately equal forces from each side.

- **Third Order Dispersion**

Dispersion in fibers is usually described by taking the lowest order term in a group velocity dispersion (GVD) expansion. In most cases, this term is dominant and the first order expansion is a good approximation. However, near the zero point of dispersion, the next term in the expansion, known as third order dispersion can be of comparable magnitude to the lowest order term, and must be considered [12]. This effect has attracted attention recently because it can be a significant effect in a dispersion-managed system, where the fiber alternates between being dispersive and anomalously dispersive and the average dispersion is slightly anomalously dispersive and very small [21]. In general, this effect is small unless the soliton frequency is very near the zero of dispersion (β_2) for the fiber.

- **Polarization mode cross coupling**

Even in a single mode optical fiber, two polarization modes can be maintained. Dispersion between these two modes is known as Polarization Mode Dispersion (PMD.) The internal structure of a soliton is very stable under the effects of PMD. However, the different polarization modes most often have different linear and non-linear indexes of refraction and therefore travel at different group velocities. Over a long span of fiber, even a pulse that starts initially in one polarization mode may be split into both modes via PMD and therefore reach the end of the fiber at different times. In addition, noise involved in PMD causes a soliton timing jitter [12] [22].

C. Design issues and performance

Careful design can help control the various sources of noise listed above. The Raman self frequency shift

and soliton-soliton interactions can be limited by using relatively wide solitons (>1 ps) at a relatively low bit rate (10 Gbit/s). Also, soliton-soliton interactions can be reduced by the use of synchronous amplitude modulation [14] and perhaps amplitude variation. In addition, one can reduce the effect of soliton-soliton interactions by using the relative timing between interior bits only [20]. Third order dispersion can be made negligible by staying away from the zero of dispersion. In fact, the signal in this model depends on the solitons seeing a net dispersion as they transit the loop. Polarization mode cross coupling can be reduced through the use of polarization maintaining (PM) fiber in the loop. However, it would increase the fiber cost substantially if a large fraction of the loop were constructed with PM fiber. Some of the effect of polarization mode cross coupling can be removed by making a differential measurement. In this model it would be necessary to place polarization controllers in strategic locations throughout the circuit. In addition, it might be possible to use polarization specific filtering and detection or make use of trapped or vector solitons (where the two polarization modes have the same group velocity) [12].

Even taking into consideration proper design, there will exist residual relative timing jitter and shifts from the noise sources above. We can place a reasonable limit on the size of the random jitter by noting the results of previous bit storage experiments. Nazakawa et al. established long-term storage of 24 ps wide solitons at 10 Gbit/s [14]. Numerous other groups have transmitted soliton bit patterns for shorter distances at higher (20-160 Gbit/s) rates [11]. Liao and Agrawal have shown through numerical simulations that it should be possible to limit the jitter to approximately 1 ps at a rate of 40 Gbit/s [23]. Based on these results, it seems reasonable to assume the random jitter can be controlled to better than the 10 ps level. This corresponds to an uncertainty in the pulse position at detection of approximately 2 mm.

Now, let us return to our experimental model and consider only noise that can cause random jitter. A 10 Gbit/s soliton beam propagating in a fiber with $D=+15$ ps/nm-km ($\beta_2 = -19$ ps²/km) is split into two streams. One travels vertically a distance h and is injected into a fiber optic storage ring, while the other is injected into a similar fiber optic storage ring at the height of the original soliton pulse source. There will be a gravitationally-induced shift in the group velocity of the solitons that move vertically, according to equation (9). If the storage rings are constructed of similar fiber (assume $D=+15$ ps/nm-km, SMF-28 fiber), the average, relative group velocity difference between the streams of solitons traveling in the two storage rings will remain. Over a storage time T , the light will travel a distance d in the storage loops and the group velocity difference will induce a relative shift in the length traveled along the two paths (in meters) of

$$\delta d = 1 \times 10^{-10} h T. \quad (26)$$

Signal vs. Storage Time for Various Height Differences

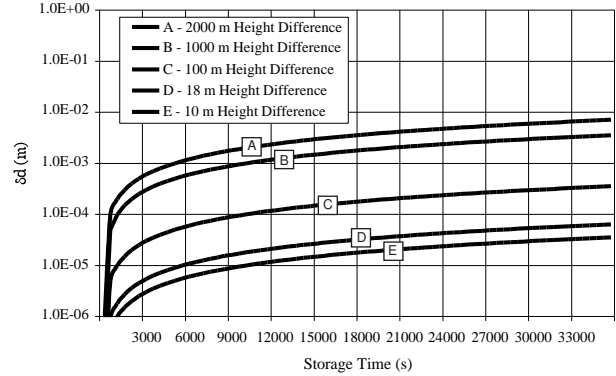


FIG. 7. Difference in travel distance between pulses in vertically separated storage loops as a function of storage time.

Limit on α vs. Storage Time

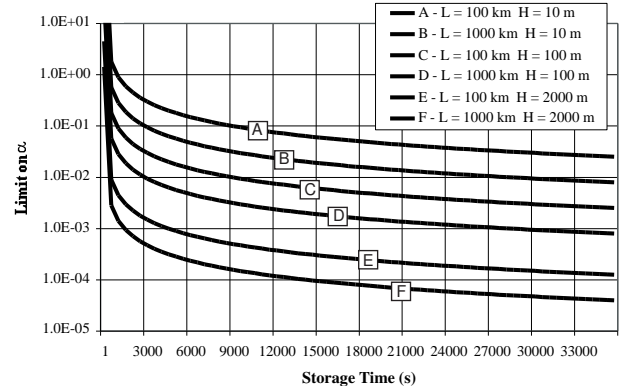


FIG. 8. Sensitivity to α as a function of storage time for various parameters of the two storage loop scheme.

There will be

$$N = \frac{\ln(\text{rate})}{c} = 50L \quad (27)$$

solitons in each storage ring of length L , assuming the rings are filled. The statistical average error on the relative position of solitons in one ring as compared to the other when the beams are recombined is

$$\delta s = \frac{0.002}{\sqrt{N}} \text{ meters.} \quad (28)$$

Figure 7 shows δd as a function of vertical loop separation d , and storage time T . The sensitivity to α , given by $\delta s/\delta d$, is plotted in Figure 8. This figure shows an interesting limit on α can be achieved under circumstances where only random jitter noise effects are considered.

Unfortunately, unidirectional soliton timing shifts within each ring are unavoidable and quite large. How-

ever, so long as these shifts are reproducible and consistent for a given ring, it should be possible to extract the gravitationally-induced timing shift using differential measurements between different loop heights. Our conceptual design creates a stable environment for the storage loops in hopes of achieving this reproducibility.

Figure 9 illustrates the basic concept of making differential measurements in this experimental model. The fiber storage rings are constructed as “modules” that can be moved carefully from place to place without disturbing the active elements of the storage loop or the environment that surrounds them. Fiber leads to and from each module are detachable, so the relative spatial configuration of the two modules can be changed in order to make differential measurements. Between separate differential measurements there will be relative changes in the input and output fibers. However, the light spends the vast majority of the storage time inside the loop. The input and output fibers constitute an extremely small fraction of the total path length, and will have a correspondingly small effect on the pulse timing.

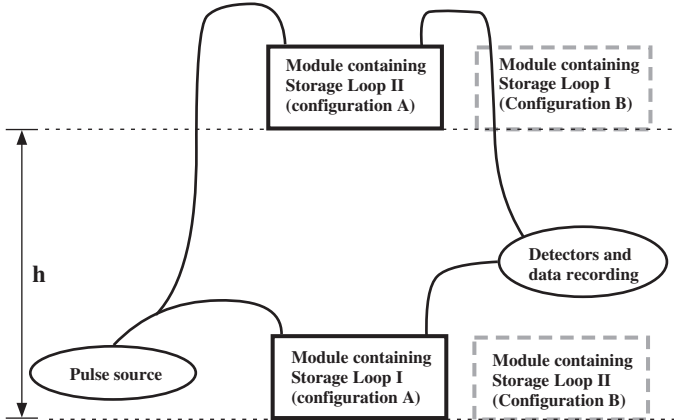


FIG. 9. The basic concept of the two storage loop differential measurement.

Figure 10 shows the basic layout of the experimental optical circuit in more detail. The source and both storage rings (and detectors, if required) are in stable environments. The ring modules are constructed to be identical, and can be disconnected and moved to different heights, as needed. Systematic effects, such as those arising from small differences between the modules/storage rings, can be taken out with differential measurements. Each pass around the ring, a small fraction of the power is picked off so that the relative timing in the two rings can be compared.

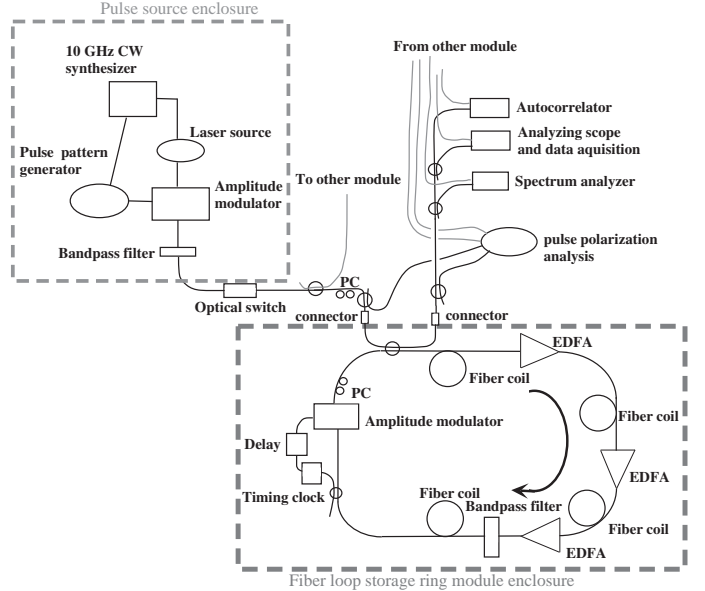


FIG. 10. Conceptual design of the optical circuit.

Figure 11 shows one concept of a fiber optic storage ring module. It consists of the basic storage ring components (fiber, bandpass filter, EDFA, and amplitude modulator) in a thermally isolated compartment that can be moved as needed. The fiber is coiled on spools that have low thermal expansion coefficients. The coils are arranged so the net area subtended by the loop is very small. This will reduce any effects due to the rotation of the earth during the measurement.

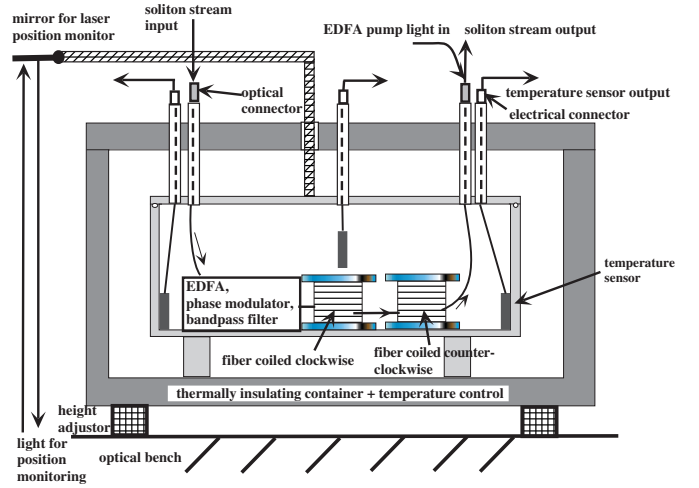


FIG. 11. Conceptual design of a fiber optic storage ring module.

The module is placed in a carefully controlled, stable thermal environment. The temperature inside the module is carefully monitored. If necessary, this information can be used for a feedback system to keep the temperature stable over time. The absolute accuracy of the temperature sensors is not critical. However, they need

to give reliable relative measurements over time.

All wires and fibers leading into the module are detachable, so the modules can be exchanged with ease, without disturbing the active elements of the loop. The items inside the module are secured so that minor movements of the module leave no net change in the positions or stresses inside the module.

A careful survey is done to locate the modules with respect to each other and to positions where measurements of the local gravitational field strength are done using a reasonably accurate gravimeter (good to 1 part in 10^6 or 10^7).

Each module rests on a stable optical table. The relative position of the two modules is monitored during a store via an interferometric system (or repeated optical surveys if such a system is simpler and more cost effective). Significant changes, perhaps due to diurnal variation in the building, can be taken out via small, remote control, height adjusters located underneath one of the modules. If necessary, these adjustments could be made automatically with feedback from the interferometric system. Accuracy on the order of 200 microns should be achievable and sufficient.

The change in the group velocity, and therefore the signal size, is directly proportional to the group velocity dispersion in the fiber loop. It is necessary to measure this dispersion as precisely as possible so it does not limit the measurement precision on α . Measurements of fiber chromatic dispersion to ± 0.02 ps/nm-km have been reported [24]. Fujise *et al.* use a wavelength-division-multiplexing (WDM) phase shift method which compares the relative phase shift between modulated light of different wavelengths passing through the fiber simultaneously. They achieve a measurement stability of ± 0.02 ps/nm-km over a ten-hour period. We will need to improve on this precision, or develop the ability to correct for changes over time using this (or a similar) technique in situ as a monitor. Another method we are considering is to send separate soliton pulses with different carrier frequencies through the loop and look at the relative timing between the pulses before and after the loop. The stability of our dispersion measurement is intimately tied in with the stability of the overall timing at the end of a store and our ability to extract the gravitational effect using differential measurements.

D. Potential for a flight project

Since the signal size of the soliton ring model depends linearly on the height difference of the two loops in a given gravitational field, it is desirable to make this quantity as large as possible. To this end, it is interesting to explore the potential gains and difficulties that might be encountered performing the soliton storage ring experiment in orbit on the space shuttle, or the International Space Station. In such an experiment, one storage loop

would remain on the shuttle/station, while the other loop would be transported to an orbit with a different radius or height, but the same angular velocity. In this scheme, loop height differences of tens of kilometers or more could be achieved.

The acceleration due to gravity in orbit will differ from that on the surface of the earth by about 10%. (The value of g is around 8.94 m/s^2 at an altitude of 160 nautical miles, which is the altitude of STS-101.) This comes in the signal with a linear dependence and must be taken into account for an exact calculation. However, for simplicity, we will ignore this difference, along with the change in g as a function of height along the loop. In practice, these ($O(10\%)$) effects must be measured and taken into account. With this simplification, equation (14) is still valid. Figure 12 shows the potential sensitivity to α for heights of 10, 20, and 50 km, respectively.

Conceptually, one module remains on the shuttle (or space station), while the other is ensconced in a small, unmanned vehicle that contains environmental control, power for EDFA pump lasers and thermal control, environmental monitoring, devices capable of relating the exact position of the one module with respect to the other, and minor propulsion and navigational capability for stability (and possible maneuvering, though perhaps this is better done by the shuttle). The two modules must be tethered together by the fibers that carry the soliton stream to and from the second module. The fibers should be surrounded by a thin, flexible covering that evens out the azimuthal asymmetry in the thermal environment and provides some degree of stress relief.

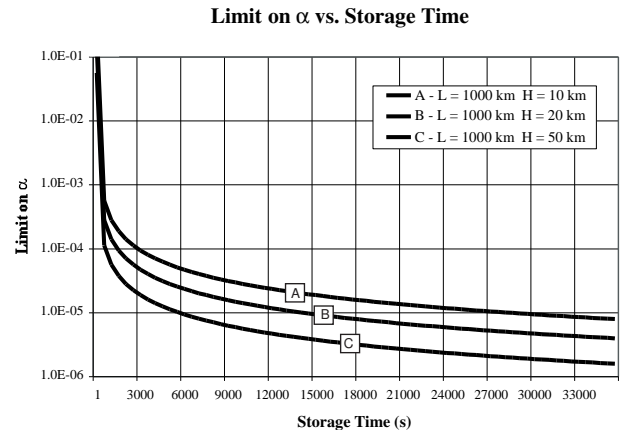


FIG. 12. Potential sensitivity to α for different loop separations in a space-based experiment.

Conceivably, the solitons could be generated separately on the two modules with the timing communicated via light pulses sent back and forth. This has the advantage of removing the need for the fiber tether and allowing the possibility of a greater height difference, and perhaps a sensitivity to higher-order terms. Unfortunately, this

raises a host of other issues, such as relative differences in the loop soliton sources and gravitational effects on the clock rate of electronics that communicates between the modules.

It is also important to note that the primary elements of this experiment are small, light, and mechanically robust. In addition, the experiment requires a relatively modest amount of power. As such, it could be flown on a variety of platforms.

This experimental model is quite novel. It would have very different systematic errors than the clock-in-space experiments that are underway.

V. CONCLUSIONS

The interplay of optical dispersion and the frequency shift of light due to a changing gravitational potential can be used to test the equivalence principle for gravitation by converting the frequency shift into a phase shift or time delay. It is possible an experiment using solitons in optical fiber storage loops could be performed that uses this effect to make a high precision measurement of the gravitational redshift of light.

VI. ACKNOWLEDGEMENTS

We are indebted to the following people for useful discussions: Govind Agrawal, Robert Boyd, Jeffrey Clark, Turan Erdogan, Alan Evans, John Heebner, Daniel Kerr, Jeff Korn, Taras Lakoba, Adrian Melissinos, John Moores, Q Han Park, Michael Perlmutter, Sarada Rajeev, and Ram Yahalom. This work was supported by the University of Rochester.

VII. REFERENCES

- [1] C.M. Will, *The Confrontation between General Relativity and Experiment: A 1998 Update*, gr-cq/9811036.
- [2] A possible exception is a neutron interference experiment that exhibits a discrepancy between the experimental and theoretical results, reported in K.C. Littrell, B.E. Allman, and S.A. Werner, Phys. Rev. **A56**, 1767 (1997).
- [3] M. Gasperini, Phys. Rev. **D38**, 2635 (1988); A. Halprin, C.N. Leung, and J. Pantaleone, Phys. Rev. **D53**, 5365 (1996); S.W. Mansour and T.K. Kuo, Phys. Rev. **D60**, 097301-1 (1999); A.M. Gago, H. Nunokawa, and R. Zukanovich Funchal, LANL preprint archive, hep-ph/99099250 (1999).
- [4] J. Jaffe, R.F.C. Vessot, Phys. Rev. **D14**, 3294 (1976); R. Hughes, Phys. Rev. **D 41**, 2367 (1990); T. Krisher, Phys. Rev. **D53**, R1735 (1996).
- [5] R.F.C. Vessot et al., Phys. Rev. Lett. **45**, 2081 (1980). See also reference [1].
- [6] See, for example, the following papers and references within: C. Shi, *A novel pulsed fiber-optic rotation sensor with opto-electronic feedback*, Optics Communications, 131 (1996), p. 47; K. Hotate, *Fiber optic gyros put a new spin on navigation*, Photonics Spectra, April 1997, p. 108; W.K. Burns, *Fiber optics, light is better*, Optics and Photonics News, May 1998, p. 28.
- [7] Kenneth McCoy, Ph.D. thesis, Georgia Institute of Technology, 1996; Taras Lakoba, University of Rochester, private communication.
- [8] M. Perlmutter, R. Yahalom, Fibersense Technology Incorporated, Canton, MA, private communication, Feb. 2000.
- [9] The factor of 100 estimate was provided by Robert Boyd, University of Rochester, private communication, April 2000.
- [10] See, for example, G. Agrawal, *Non-linear fiber optics*, 2nd edition, Academic Press, 1995 or Y.S. Kivshar and B. Luther-Davies, Phys. Rep. **298** (1998) 81.
- [11] A good review containing many references to fiber storage loops is H. Haus and W. Wong, Rev. Mod. Phys. **68** (1996) 423.
- [12] G. Agrawal, *Non-linear fiber optics*, 2nd edition, Academic Press, 1995.
- [13] This is somewhat similar to a continuous wave experiment suggested in J. Anandan, Phys. Rev. **D15** (1977) 1448 and neutron interference experiments reported in R. Colella, A.W. Overhauser, S.A. Werner, Phys. Rev. Lett. **34** (1975) 1472.
- [14] M. Nakazawa et al., Electronics Letters, Vol. 29 (1993) 729.
- [15] J.P. Gordon and H.A. Haus, Opt. Lett. **11**, 665 (1986).
- [16] H.A. Haus and A. Mecozzi, Opt. Lett. **17**, (1992) 1500; J.D. Moores, W. Wong, H.A. Haus, Opt. Comm. **113** (1994) 153.
- [17] J.P. Gordon, Optics Lett. **11**, 662 (1986).
- [18] F.M. Mitschke and L. F. Mollenauer, Optics Lett. **11**, 659 (1986).
- [19] C. Desem and PL Chu, IEEE Proc. **134**, Pt. J, 145 (1987).
- [20] A.N. Pinto, G.P. Agrawal, and J. Ferreira De Rocha, Journal of Lightwave Technology **16** (1998) 515.
- [21] K. Hizanidis et al., Pure Appl. Opt. **7** (1998) L57; T. I. Lakoba and G.P. Agrawal, J. Opt. Soc. Am. B **16** (1999) 1332.
- [22] L.F. Mollenauer and J.P. Gordon, Opt. Lett. **19** (1994) 375.
- [23] Z.M. Liao and G.P. Agrawal, IEEE Photonics Technology Letters **11** (1999) 818.
- [24] B. Christensen et al., Elect. Lett. **23** (1987) 357; M. Fujise et al., J. Lightwave Tech. **LT-5** (1987) 751.